Optimal Operation of Energy Hub Based Micro-energy Network with Integration of Renewables and Energy Storages

Thanhtung Ha, Ying Xue, Kaidong Lin, Yongjun Zhang, Vu Van Thang, and Thanhha Nguyen

***Abstract*—This study proposes an optimized model of a micro-energy network (MEN) that includes electricity and natural gas with integrated solar, wind, and energy storage systems (ESSs). The proposed model is based on energy hubs (EHs) and it aims to minimize operation costs and greenhouse emissions. The research is motivated by the increasing use of renewable energies and ESSs for secure energy supply while reducing operation costs and environment effects. A general algebraic modeling system (GAMS) is used to solve the optimal operation problem in the MEN. The results demonstrate that an optimal MEN formed by multiple EHs can provide appropriate and flexible responses to fluctuations in electricity prices and adjustments between time periods and seasons. It also yields significant reductions in operation costs and emissions. The proposed model can contribute to future research by providing a more efficient network model (as compared with the traditional electricity supply system) to scale down the environmental and economic impacts of electricity storage and supply systems on MEN operation.**

***Index Terms*—Micro-energy network (MEN), natural gas price, electricity price, energy hub (EH), renewables, energy storage optimal operation.**

I. Introduction

EXHAUSTION of traditional energy resources and the problems posed by environmental pollution are two major issues that the modern world must address. In the past, different forms of energy such as electricity, heat, and cooling often existed as single stand-alone systems [1]. In recent years, researchers have turned their focus to optimal combinations of these types of energy because of the benefits presented in [2], [3]. Different forms of energy can be transformed and be mutually supportive in energy networks [4]-[6]. In terms of energy costs, households may choose different low-cost energy forms to meet their energy needs. In general, the goal of an energy network is to satisfy two economic factors and meet the energy needs of consumers. This model enhances reliability, reduces environmental pollution, promotes the development of optimal energy-consuming systems, enhances stability, and achieves the goals of using economical and efficient energy.

The energy hub (EH) is a concept that was introduced in [1] and has attracted considerable interests from researchers. EH was considered as a versatile system that combines power and load through a converter system [7], [8]. A series of studies [9]-[11] previously addressed issues related to EH and the relationships among different forms of energy through the EH model. In general, an EH provides an optimal combination of various forms of energy, which can then be used for storage, distributed energy resources (DERs), electric vehicles, etc. With these advantages, energy network models that include different forms of energy through EH have been studied. An energy network model is formed from relatively small, diversified EHs that are applied to residential areas, where a greater scale may be applied to a nation as a whole.

The study in [12] constructed a test system of 11 EHs in a multi-carrier energy system to solve the optimization problem of power flow in the system. The study in [13] analyzed an energy network including three EHs. The results showed that the system could meet node voltage stability, reduce losses on the power grid, and reduce the cost of converting gas into electricity. The studies in [14] and [15] optimized an energy network consisting of multiple EHs considering the voltage limits of the power grid. Results showed that the price band was lowered, the electricity was successfully converted, and the losses of the entire system were reduced.

With the emergence and development of energy networks and EHs, renewable energy and energy storage technologies are two additional solutions that have been extensively studied. Traditional energy distribution through an electricity network has been shown to have greater energy efficiency and operation when these two solutions are applied [16]. However, fully exploiting applications from renewable energies remains primarily in the form of electric power, and heat has

Manuscript received: March 24, 2020; revised: July 19, 2020; accepted: August 17, 2020. Date of CrossCheck: August 17, 2020. Date of online publication: November 20, 2020.

This work was supported by the National Natural Science Foundation of China (No. 51777077) and Thai Nguyen University of Technology (TNUT), Thai Nguyen, Vietnam.

T. Ha (corresponding author) and V. V. Thang are with the Department of Electric Power Systems, Thai Nguyen University of Technology (TNUT), Thai Nguyen, Vietnam (e-mail: tunganh@tnut.edu.vn; thangvvhtd@tnut.edu.vn).

Y. Xue is with University of Birmingham, Birmingham, U. K. (e-mail: y.xue@bham.ac.uk).

K. Lin and Y. Zhang are with the School of Electric Power, South China University of Technology, Guangzhou, China (e-mail: 596875439@qq.com; zhangjun@scut.edu.cn).

T. Nguyen is with Thai Nguyen University, Thai Nguyen, Vietnam (e-mail: hant@tnu.edu.vn).

DOI: 10.35833/MPCE.2020.000186

been rarely discussed. Some previous studies have evaluated the efficiencies of renewable energies and energy storage systems (ESSs) in relation to the independent EH optimization problem [17]-[20]. However, the impact of energy network models formed by multiple EHs on energy systems has not been adequately assessed. The new operation problems are solved only within the context of optimizing power flow between EHs and without comparing the concrete efficiencies of energy networks and traditional electricity networks.

Previous studies have shown that cooling, heat, and power systems for residential areas can be used as standard EH models [7], [17], [18]. In large areas, energy networks must supply the loads that are separated by large distances. Therefore, to supply energy to customers, many EHs are connected to large-scale EH networks by distribution networks. The operation through multiple EHs has been discussed in [21]-[29]. However, these studies have not fully addressed the optimization problems with multiple EHs. They have also failed to consider the integration of storage and regeneration systems and to assess their ability to solve operation problems. Table I summarizes model parameters evaluated in previous research and in this study, where C_1, C_2, and C_3 are the total energy cost, total energy loss cost, and total emission cost, respectively; SHE, ES, CS, TS, PV, and WP stand for solar heat exchanger, electricity storage, cooling storage, thermal storage, photovoltaic, and wind power, respectively; and √ represents that the corresponding item is considered.

TABLE I
COMPARISONS OF PROPOSED AND PREVIOUS MODELS BASED ON ENERGY SYSTEM PARAMETERS

Reference	Objective function			DER			ESS		
	C_1	C_2	C_3	WP	PV	SHE	ES	CS	TS
[7]	√			√	√	√	√		
[8], [17]-[20], [30]	√			√	√	√	√	√	√
[9]	√			√	√			√	√
[10], [26], [27], [31]	√	√	√	√	√		√		√
[11]	√			√	√		√	√	√
[12]-[15]	√			√					
[16]	√				√		√		
[21], [28]	√		√				√		
[22]	√			√	√		√		√
[23]	√			√			√	√	√
[24]	√								
[25]	√	√		√			√		√
[29]	√			√	√		√		
[32]	√						√		√
Proposed model	√	√	√	√	√	√	√	√	√

Major contributions of this study are as follows.

1) This study analyzes the problems of optimizing operation costs in the micro-energy network (MEN) with EHs and integrating renewable energies in ESSs and distribution networks by applying mixed-integer nonlinear programming.

2) This study presents the way of achieving optimal operations of the MEN in four operation cases by considering various operation parameters and energy losses in both electricity and natural gas distribution networks.

3) This study assesses the impact of energy sources and energy storage equipment on MEN performance by measuring system energy consumption and emissions across four operation cases.

The EH can be considered as a grand network node that incorporates different forms of energy. The demands for electricity, heat, and cooling loads can be fulfilled by using conversion and storage devices. This study presents four operation cases to evaluate how energy sources and storage systems affect an MEN. The MEN assessed in this study is based on a 10 kV power distribution network with six load nodes. Solar, wind, and ESSs are considered in the case studies.

The remainder of this paper is organized as follows. The concept, structure, and mathematical descriptions of the EH model are described in Section II. Section III discusses energy balance and the MEN system structure in relation to electricity and natural gas networks. Section IV formulates the optimal operation problem for an MEN with the objective function of minimizing energy costs and reducing greenhouse emissions derived from the use of natural gas. Section V describes how we solve the optimal operation problem using general algebraic modeling system (GAMS). The MEN optimization problem is considered with four configurations that simultaneously meet the demands for cooling, heat, and power with six additional load nodes. Finally, Section VI presents the conclusion and discusses the future work.

II. CONCEPT, STRUCTURE AND MATHEMATICAL DESCRIPTION OF EH MODEL

The concept and structure of the EH were previously described in [30]. The EH uses energy-centric routers and optimally converts energy to electricity, heat, and cooling, etc. The goal of the EH is to convert energy sources so as to increase energy efficiency and promote rationality and environmental friendliness while meeting the diverse demands of energy consumers. In general, an EH is considered as a node in an energy network with multiple inputs and outputs. Figure 1 presents the topology of an EH, in which different forms of energy are represented, where P and L denote the input energy and output energy, respectively; and α, β, ω represent energy types such as natural gas and electricity. The EH model has n conversion devices with efficiencies of $\eta_1, \eta_2, \ldots, \eta_n$.

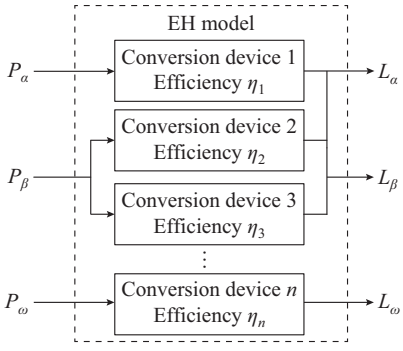

Fig. 1. Topology of EH.

III. System Modeling

A. MEN Based on EH

An MEN extends the concept of a microgrid and can be considered as a small-scale regional power distribution network with an innovative topology and configuration. It is suitable for households in urban areas, which has some advantages. From a power-supply perspective, MEN can promote new and renewable energy applications, particularly solar applications (e. g., PV and solar thermal), wind energy combined with natural gas, electricity, and other forms of energy. In terms of energy-service supply, an MEN can reduce energy costs and emissions, and cut down on additional loads while simultaneously accommodating the diversity of loads. Regarding the energy network structure, the coordinated operation of electricity and natural gas networks can promote diversified and sustainable development of energy technologies. With these advantages, this study proposes an MEN model formed by multiple EHs to link electricity and natural gas networks, as shown in Fig. 2.

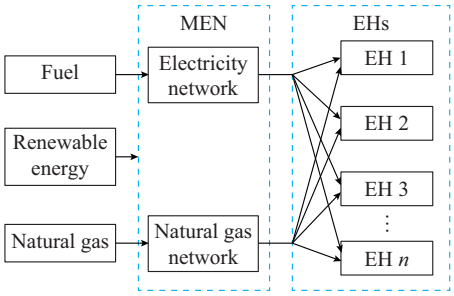

Fig. 2. Structure of MEN model based on EHs.

B. Electricity Network

A power distribution network can be expressed through the active power and reactive power basic nodes, which are given as:

$$P_{\mathrm{E},i}^{\mathrm{G}}=P_{\mathrm{E},i}^{\mathrm{D}}+V_i\sum_{j=i}^{n_{\mathrm{E}}}V_j\left(G_{\mathrm{E},ij}\cos\theta_{ij}+B_{\mathrm{E},ij}\sin\theta_{ij}\right) \tag{1}$$

$$Q_{\mathrm{E},i}^{\mathrm{G}}=Q_{\mathrm{E},i}^{\mathrm{D}}+V_i\sum_{j=i}^{n_{\mathrm{E}}}V_j\left(G_{\mathrm{E},ij}\sin\theta_{ij}-B_{\mathrm{E},ij}\cos\theta_{ij}\right) \tag{2}$$

where V_i and V_j are the voltages of the buses i and j, respectively; n_{E} is the number of buses in the electricity network; $P_{\mathrm{E},i}^{\mathrm{G}}$ and $Q_{\mathrm{E},i}^{\mathrm{G}}$ are the active and reactive power generations, respectively; $P_{\mathrm{E},i}^{\mathrm{D}}$ and $Q_{\mathrm{E},i}^{\mathrm{D}}$ are the active and reactive load demands, respectively; $G_{\mathrm{E},ij}$ and $B_{\mathrm{E},ij}$ are the conductance and susceptance between buses i and j, respectively; and θ_{ij} is the phase angle between buses i and j.

C. Natural Gas Network

Pipeline gas flow can be calculated from the pressure at both pipe ends and the pipe parameters given in [33], [34]:

$$f_{ij}^{\mathrm{L}}=k_{ij}^{\mathrm{L}}\cdot sign\left(p_i,p_j\right)\cdot\sqrt{sign\left(p_i,p_j\right)\left(p_i^2-p_j^2\right)} \tag{3}$$

where f_{ij}^{L} and k_{ij}^{L} are the natural gas flow and gas pipe coefficient from bus i to bus j, respectively; p_i and p_j are the gas pressures at buses i and j, respectively; and $sign\left(p_i,p_j\right)$ is the direction of flow in the gas pipeline. Its specific values are determined by:

$$sign\left(p_i,p_j\right)=\begin{cases}1 & p_i>p_j\\ -1 & \text{otherwise}\end{cases} \tag{4}$$

Because of the decrease in gas pressure along with its transmission, it is necessary to allocate compressors to ensure sufficient gas pressure. Two types of compressors exist: gas-fired and electric. In this study, we assume all compressors are air compressors that consume natural gas. Natural gas flow can be described by:

$$f_{ij}^{\mathrm{C}}=k_{ij}^{\mathrm{C}}f_{ij}^{\mathrm{L}}\left(p_j-p_i\right) \tag{5}$$

where k_{ij}^{C} is the constant of the compressor; and f_{ij}^{C} is the pressure drop from bus i to bus j.

Natural gas flow can be calculated based on the natural gas flow in the pipeline and gross heat value GHV of the natural gas as:

$$\begin{cases}P_{\mathrm{G},ij}^{\mathrm{L}}=GHV\cdot f_{ij}^{\mathrm{L}}\\ P_{\mathrm{G},ij}^{\mathrm{C}}=GHV\cdot f_{ij}^{\mathrm{C}}\end{cases} \tag{6}$$

where $P_{\mathrm{G},ij}^{\mathrm{L}}$ and $P_{\mathrm{G},ij}^{\mathrm{C}}$ are the capacities of natural gas and pressure pumps from bus i to bus j, respectively.

Then, the gas equilibrium equation can be written as:

$$P_{\mathrm{G},i}^{\mathrm{S}}=P_{\mathrm{G},i}^{\mathrm{D}}+\sum_{j=1}^{n_{\mathrm{G}}}P_{\mathrm{G},ij}^{\mathrm{C}}+\sum_{j=1}^{n_{\mathrm{G}}}P_{\mathrm{G},ij}^{\mathrm{L}} \tag{7}$$

where $P_{\mathrm{G},i}^{\mathrm{S}}$ is the capacity of natural gas flowing into bus i; $P_{\mathrm{G},i}^{\mathrm{D}}$ is the natural gas capacity attained at bus i; and n_{G} is the number of nodes in the natural gas network.

IV. Optimal Operation Models

A. Proposed Model

1) MEN Modeling

This study proposes a structured MEN model, as shown in Fig. 3.

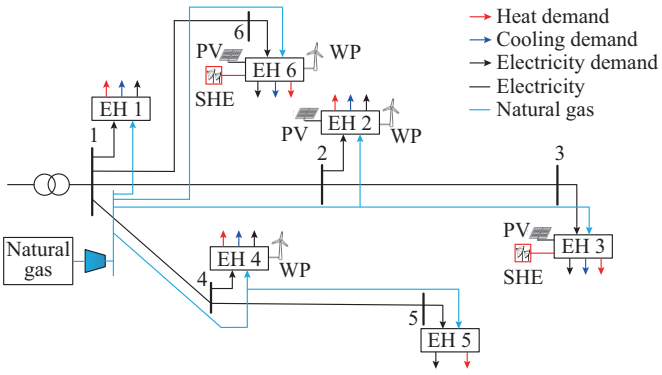

Fig. 3. Structured MEN model.

An MEN is formed based on a microgrid with a voltage of 10 kV that meets the demands for electricity, heat, and cooling of six additional loads. Natural gas and electricity networks are connected through EHs. Within the framework of the research model, applications from solar energy (can

be exploited in the form of electricity through solar thermal and electricity via PV systems), WP, and electricity, heat, cooling storage systems are equipped in EHs. The proposed model demonstrates how to meet diverse energy needs of loads using electricity (from distribution systems, solar panels, and wind turbines) and heat (from an SHE network). EESs play the role of charging and discharging according to the optimal operation mode of the MEN.

2) Structures of EHs

The structure of each EH in the MEN greatly influences the optimal operation of the MEN. The structures of EHs must ensure the connection between the input energy elements (from the power distribution network, natural gas network, solar and WP) and the output energy elements including electricity, heat, and cooling.

A general EH structure consists of 12 devices, as shown in Fig. 4. In particular, the input energy for an EH includes the energy from the power distribution network, natural gas network, and decentralized energy generations (wind and solar). The conversion equipment includes the voltage transformer (T), micro turbine (MT), air conditioner (AC), gas boiler (GB), absorption chiller (ACh), SHE, and electric heater (EHe). The storage system group contains ES, TS, and CS. Demands for energy include additional loads, heat, and cooling.

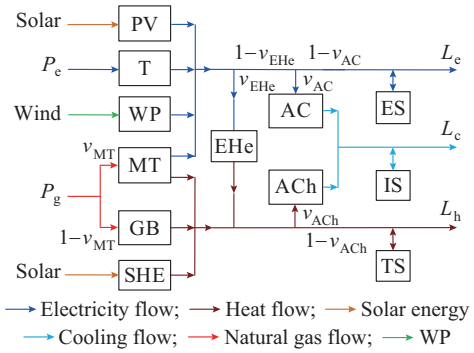

Fig. 4. General EH model.

The MEN consists of six EHs corresponding to $n=n_e=n_g=1,2,\ldots,6$. The parameters in the energy equation of the EH at the n^{th} node are described as follows. The output power of EH n consists of $L_{e,n}(t)$, $L_{h,n}(t)$, and $L_{c,n}(t)$, which are the demands for electricity, heat, and cooling of loads, respectively. $P_{e,n}(t)$ and $P_{g,n}(t)$ are the input power of EH n for electricity and natural gas, respectively. $\eta^{T}_{e,n}$, $\eta^{MT}_{ge,n}$, $\eta^{MT}_{gh,n}$, $\eta^{GB}_{h,n}$, $\eta^{AC}_{e,n}$, $\eta^{ACh}_{h,n}$, and $\eta^{EHe}_{h,n}$ are the conversion performances of the T_n, MT_n, GB_n, AC_n, ACh_n, and EHe_n, respectively. $v_{AC,n}(t)$, $v_{MT,n}(t)$, $v_{ACh,n}(t)$, and $v_{EHe,n}(t)$ are the conversion rates of the devices AC_n, MT_n, ACh_n, and EHe_n, respectively (these are also considered as the dispatching ratios of electricity, natural gas, and heat conversion, respectively). $P^{PV}_{e,n}(t)$, $P^{WP}_{e,n}(t)$, and $P^{SHE}_{h,n}(t)$ are the discharging power capacities of the PV, WP, and SHE, respectively. The charging and discharging power of the ES, TS, and CS devices are denoted by $P^{dis}_{ES,n}(t)$, $P^{ch}_{ES,n}(t)$, $P^{dis}_{HS,n}(t)$, $P^{ch}_{HS,n}(t)$, $P^{dis}_{CS,n}(t)$, $P^{ch}_{CS,n}(t)$, respectively.

$$L_{e,n}(t)=\left(P_{e,n}(t)\eta^{T}_{e,n}+P_{g,n}(t)v_{MT,n}(t)\eta^{MT}_{ge,n}+P^{WP}_{e,n}(t)+P^{PV}_{e,n}(t)\right)\cdot \left(1-v_{EHe,n}(t)\right)\left(1-v_{AC,n}(t)\right)+P^{dis}_{ES,n}(t)-P^{ch}_{ES,n}(t) \quad (8)$$

$$L_{h,n}(t)=\left\{P_{g,n}(t)\left[v_{MT,n}(t)\eta^{MT}_{gh,n}+\left(1-v_{MT,n}(t)\right)\eta^{GB}_{h,n}\right]+P^{SHE}_{h,n}(t)+P_{e,n}(t)\eta^{T}_{e,n}+P_{g,n}(t)v_{MT,n}(t)\eta^{MT}_{ge,n}+P^{PW}_{e,n}(t)+P^{PV}_{e,n}(t)\right\}\cdot \eta^{EHe}_{h,n}v_{EHe,n}(t)\left(1-v_{ACh,n}(t)\right)+P^{dis}_{HS,n}(t)-P^{ch}_{HS,n}(t) \quad (9)$$

$$L_{c,n}(t)=\left\{P_{g,n}(t)\left[v_{MT,n}\eta^{MT}_{gh,n}+\left(1-\sigma_{MT,n}\right)\eta^{GB}_{h,n}\right]+P^{SHE}_{h,n}(t)+\left(P_{e,n}(t)\eta^{T}_{e,n}+P_{g,n}(t)v_{MT,n}(t)\eta^{MT}_{ge,n}+P^{WP}_{e,n}(t)+P^{PV}_{e,n}(t)\right)\eta^{EHe}_{h,n}v_{EHe,n}(t)\right\}\cdot v_{ACh,n}\eta^{ACh}_{h,n}+\left(P_{e,n}(t)\eta^{T}_{e,n}+P_{g,n}(t)v_{MT,n}(t)\eta^{MT}_{ge,n}+P^{WP}_{e,n}(t)+P^{PV}_{e,n}(t)\right)\left(1-v_{EHe,n}(t)\right)v_{AC,n}(t)\eta^{AC}_{e,n}+P^{dis}_{CS,n}(t)-P^{ch}_{CS,n}(t) \quad (10)$$

Equation (8) shows that load power is provided by the electricity network through the T and the natural gas system through MT, PV, and WP. The demand for thermal energy of the load is retrieved from the natural gas system through MT and GB and from the electricity network through EHe, and the remaining heat is supplied by the solar power through SHE according to (9).

Cooling demands are met simultaneously by two AC and ACh devices, which are supplied by the electricity and natural gas networks according to (10). Binary numbers (1,0) are used to indicate the availability of all devices in the six EHs. Based on the demand for energy consumption, the structures of all six EHs are listed in Table II.

TABLE II
STRUCTURES OF SIX EHS IN MEN MODEL

EH	Availability											
	T	MT	GB	AC	EHe	ACh	PV	WP	SHE	ES	TS	IS
EH 1	1	1	1	1	0	0	0	0	0	0	0	0
EH 2	1	1	1	1	0	1	1	1	0	1	0	1
EH 3	1	1	1	1	0	1	1	0	1	1	0	0
EH 4	1	1	1	1	0	1	0	1	0	0	0	0
EH 5	1	1	1	0	1	0	0	0	0	0	0	0
EH 6	1	1	1	1	1	1	1	1	1	1	1	1

B. Mathematical Model

1) Objective Function

The optimal operation of MEN is to minimize total energy payment cost *EPC*, which includes the cost of purchasing electricity $c^{Net}_{e}(t)$ and natural gas $c^{Net}_{g}(t)$ and the total cost of greenhouse emissions generated from MT and GB devices in a day (24 hours).

$$\min EPC=\sum_{t=1}^{24}\left(P_{e,tot}(t)c^{Net}_{e}(t)+P_{g,tot}(t)c^{Net}_{g}(t)+\sum_{n=1}^{6}\sum_{em=1}^{3}c_{em}\cdot EF^{MT}_{em}\cdot P^{MT}_{g,n}(t)+\sum_{n=1}^{6}\sum_{em=1}^{3}c_{em}\cdot EF^{GB}_{em}\cdot P^{GB}_{g,n}(t)\right) \quad (11)$$

where $P_{e,tot}(t)$ and $P_{g,tot}(t)$ are the total energy of electricity and natural gas purchased from an external system at time t, respectively (considering total power loss $\sum\Delta P_e$ and total

natural gas loss $\sum \Delta P_g$ during the energy transmission); EF_{em}^{MT} and EF_{em}^{GB} are the emission factors of MT and GB, respectively; c_{em} is the emission cost; $em = 1, 2, 3$ represents the emissions of CO_2, SO_2, and NO_2, respectively; and $P_{g,n}^{MT}(t)$ and $P_{g,n}^{GB}(t)$ are the purchased power of natural gas from the network for MT and GB at time t, respectively.

2) Constraints

1) Transmission network constraints

In Section III, we introduce a mathematical model of energy balance for natural gas and electricity network using (1)-(7). In addition to the constraints previously described, other constraints of the system include the limitations to active power, reactive power, and node voltages in the electricity network and limitations to pressure and compression ratios in the natural gas network, which are represented as:

$$P_{E,i}^{G,\min} \le P_{E,i}^{G} \le P_{E,i}^{G,\max} \tag{12}$$

$$Q_{E,i}^{G,\min} \le Q_{E,i}^{G} \le Q_{E,i}^{G,\max} \tag{13}$$

$$p_i^{\min} \le p_i \le p_i^{\max} \tag{14}$$

$$V_i^{\min} \le V_i \le V_i^{\max} \tag{15}$$

$$p_{ck}^{\min} \le p_{ck} \le p_{ck}^{\max} \tag{16}$$

where superscripts max and min represent the maximum and minimum values of the corresponding variables, respectively; and p_{ck} is the compression ratio of the compressor.

2) Constraints of EHs

The constraints of energy balance for EH n is introduced by (8)-(10). Other constraints include (17), which represents constraints of the input power of electricity and natural gas in EH n ($P_{e,g,n}(t)$), and (18), which represents conversion limits for AC, MT, ACh, and EHe by state variables $v_{AC,n}(t)$, $v_{MT,n}(t)$,$v_{ACh,n}(t)$, and $v_{EHe,n}(t)$, respectively, at time t of EH n.

$$P_{e,g,n}(t) \le P_{e,g,n}^{\max} \tag{17}$$

$$v_{AC,n}(t), v_{MT,n}(t), v_{ACh,n}(t), v_{Ehe,n}(t) \in [0, 1] \tag{18}$$

3) ESS

The ESS in the MEN uses three types of storage devices, i.e., ES, TS, and CS, at EH n. Basically, the principles of their charging/discharging effects are the same. When every EH at time t is considered, the ESS is investigated through the charging/discharging process and the corresponding energy loss factor $\rho_{X,n}^{loss}$, where X represents ES, TS, or CS. Formulae (19) and (20) represent the energy stored and storage capacities of the storage devices, respectively. Equation (21) represents the energy loss during the charging/discharging process of the storage devices, and (22) represents the charging/discharging limit of the storage devices. Through binary variables $\psi_{X,n}^{ch}(t)$ and $\psi_{X,n}^{dis}(t)$, (23) represents the operation mode (charging or discharging) of the storage devices.

$$P_{X,n}(t) = P_{X,n}(t-1) + P_{X,n}^{ch}(t) - P_{X,n}^{dis}(t) - P_{X,n}^{loss}(t) \tag{19}$$

$$P_{X,n}^{\min} \le P_{X,n}(t) \le P_{X,n}^{\max} \tag{20}$$

$$P_{X,n}^{loss}(t) = \rho_{X,n}^{loss} P_{X,n}(t) \tag{21}$$

$$\begin{cases} 0 \le P_{X,n}^{ch}(t) \le P_{X,n}^{ch,\max} \\ 0 \le P_{X,n}^{dis}(t) \le P_{X,n}^{dis,\max} \end{cases} \tag{22}$$

$$\begin{cases} \psi_{X,n}^{ch}(t) P_{X,n}^{ch}(t) > 0 \Leftrightarrow \psi_{X,n}^{ch}(t) = 1 \\ \psi_{X,n}^{dis}(t) P_{X,n}^{dis}(t) > 0 \Leftrightarrow \psi_{X,n}^{dis}(t) = 1 \\ \psi_{X,n}^{dis}(t) + \psi_{X,n}^{ch}(t) = 1 \\ \psi_{X,n}^{dis}(t) \psi_{X,n}^{ch}(t) = 0 \end{cases} \tag{23}$$

where $P_{X,n}(t)$ and $P_{X,n}^{loss}(t)$ are the energy stored and energy loss of the storage devices, respectively.

The energy balance constraint in the calculation cycle T = 24 hours is expressed as:

$$P_{X,n}(0) = P_{X,n}(T) \tag{24}$$

4) Energy prices

Energy prices, including electricity and natural gas prices, are the determinants of the objective function in (4). Natural gas prices are constant [31], [32], [35]. The tariffs are determined by the time-of-use (TOU) [31]. A TOU price is the simplest form of dynamic price. The primary objective of the pricing program is to encourage less energy consumption during the peak hours.

V. Case Studies

Four operation cases for the MEN, as listed in Table III, are used to assess the effects of renewable energies (solar and wind) and ESSs on the performance of the proposed model.

TABLE III
Four Operation Cases of MEN

Case	Electricity network	Natural gas network	Solar and wind	ESS (ES, HS, CS)
1	√			
2	√	√		
3	√	√	√	
4	√	√	√	√

In all the cases, the demands for electricity, heat, and cooling of six additional loads are the same. In Case 1, because only one form of energy is used, electricity is required at the node n to convert power from heat to electricity and to cooling through EHe and AC. The structure of the EH n is shown in Fig. 5.

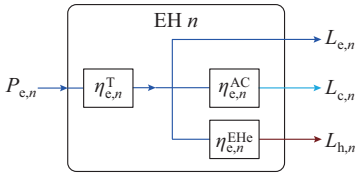

Fig. 5. Structure of EH n when using only electricity.

Then, the input power of EH n is calculated by:

$$P_{e,n}(t) = \frac{1}{\eta_{e,n}^{T}} \left(L_{e,n}(t) + \frac{L_{c,n}(t)}{\eta_{e,n}^{AC}} + \frac{L_{h,n}(t)}{\eta_{e,n}^{EHe}} \right) \tag{25}$$

A. Database

The parameters and values for the MEN shown in Fig. 3 are described as follows. The bounded power from the pow-

er system through the T is 20 MVA, the rated voltage is 10 kV, and the allowable voltage node limitation is [0.9, 1.1]p.u.. The natural gas system has a nominal capacity of 20 MW for the MEN. The base pressure of the natural gas network is 10 bar. The detailed information on the load and system parameters as well as energy prices is described in the following subsections.

1) Demand for Electricity, Heat, and Cooling

As described in Section IV-A, the MEN is designed for use in residential urban areas where the demands for electricity, heat, and cooling energy are clearly distinguished. Load parameters, including the demands for electricity, heat, and cooling, are based on the studies in [7] and [8] and presented in Fig. 6.

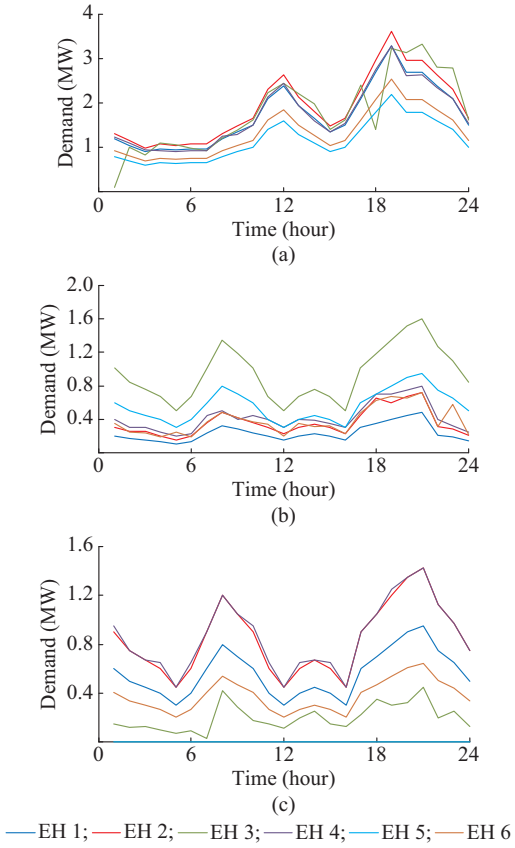

Fig. 6. Demands for electricity, heat, cooling energy in a day. (a) Electricity. (b) Heat. (c) Cooling.

2) Energy Price

Real-time energy prices are presented in Fig. 7 and are determined by the TOU price [36]. By contrast, the natural gas price is regarded as being constant [37].

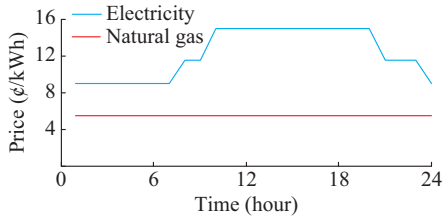

Fig. 7. Prices of electricity and natural gas.

3) Network Parameters

The parameters of the electricity and natural gas networks (the line type is YJV22-3*240**)** are presented in Table IV, whereas those of the six EHs are presented in Table V and those of emissions (CO_2, NO_2, SO_2) in [31] are adopted. In Table IV, R_E, X_E, B_E are the resistance, reactance, susceptance of the electricity network, respectively. In Table V, μ_{ES} and μ_{HS} are the storage efficiencies of the ES and HS, respectively.

TABLE IV
PARAMETERS OF ELECTRICITY AND NATURAL GAS NETWORKS

Line	Electricity network				Natural gas heating value K (s)
	R_E (Ω)	X_E (Ω)	B_E (mS)	Length (km)	
1-2	0.096	0.1080	0.1300	1.2	7
2-3	0.072	0.0810	0.0972	0.9	9
1-4	0.120	0.1350	0.1620	1.5	6
4-5	0.084	0.0945	0.1134	1.5	8
1-6	0.144	0.1620	0.1944	1.8	5

TABLE V
DEVICE PARAMETERS IN EHS

Parameter	Value	Parameter	Value
η_e^T	0.95	$P_{ES}^{ch,max}$	0.45 MW
η_{ge}^{MT}	0.40	$P_{ES}^{dis,max}$	0.45 MW
η_{gh}^{MT}	0.50	P_{ES}^{min}	0.05 MW
$\eta_{h,n}^{EHe}$	0.90	P_{ES}^{max}	4.2 MWh
η_h^{GB}	0.90	$P_{HS}^{ch,max}$	0.45 MW
η_h^{ACh}	0.85	$P_{HS}^{dis,max}$	0.45 MW
η_e^{AC}	0.80	P_{HS}^{max}	4.2 MWh
ρ_{ES}^{loss}	0.02	$P_{CS}^{ch,max}$	0.45 MW
ρ_{HS}^{loss}	0.02	$P_{CS}^{dis,max}$	0.45 MW
μ_{ES}	0.93 MW	P_{CS}^{min}	0.05 MW
μ_{HS}	0.96 MW		

To simplify computations, the output energies of PV, WP, and SHE are assumed to be the same due to the fact that wind and solar power generations are considered in all four operation cases, as shown in Fig. 8.

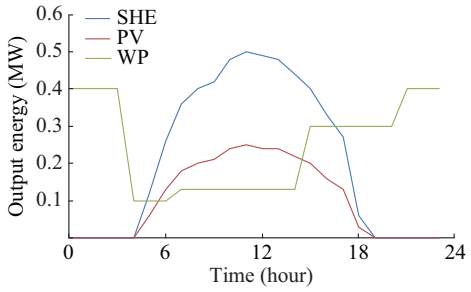

Fig. 8. Output energy of PV, SHE, and WP in a day.

B. Calculation Results

The programming language of GAMS (solver MINOS) [38] is used to analyze the MEN and conduct the optimization for integrated electricity and natural gas networks in

terms of the objective function (11) and constraints (12) - (23). The comparisons of costs in four cases are listed in Table VI.

TABLE VI
COMPARISONS OF COSTS IN FOUR CASES

Case	Total operation cost ($/day)	Total energy loss (MW)	Total loss cost ($/day)	Total emission cost ($/day)
1	52653	8.48	857	0
2	38297	5.21	721	799
3	34335	4.42	615	688
4	33782	3.38	528	589

1) Case 1

Case 1 assumes that the MEN only operates with the structure as a microgrid. Based on (24), the additional load nodes are assumed to be equipped with EHs (the structure of which is shown in Fig. 5) to meet the demands for electricity, heat, and cooling. Using the programming language of GAMS, the grid analysis consists of six additional load nodes using the electricity network parameters listed in Table IV. The electricity purchased from the system in a day is shown in Fig. 9(a). The optimal results reveal that the demand for the electricity purchased from the system during peak hours is very high, reaching a high of 29.95 MW at 7 p.m.. This can be explained by the fact that the characteristic lines of the EHs are quite similar, i. e., the demand during peak hours is high.

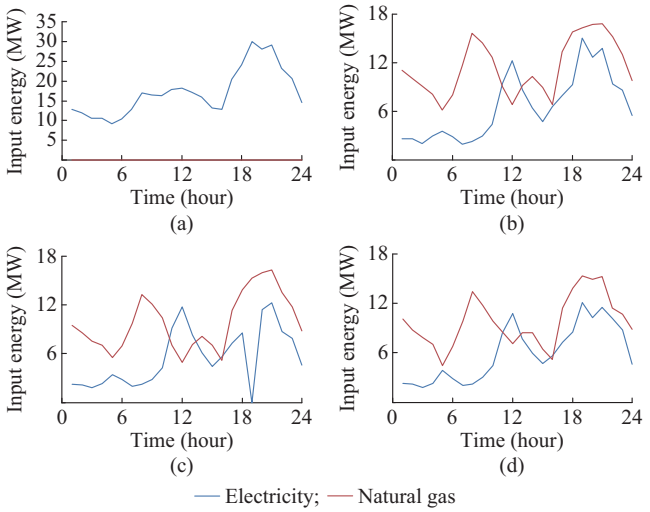

Fig. 9. Input energy of electricity and natural gas networks in four cases. (a) Case 1. (b) Case 2. (c) Case 3. (d) Case 4.

2) Case 2

The optimal operation of the MEN, including the microgrid and natural gas network (regardless of ESSs and renewable energies involved), is considered in Case 2. The input energy of the network is calculated as shown in Fig. 9(b). The results reveal that the simultaneous exploitation of the electricity and natural gas networks dramatically change the demand for electricity. Compared with Case 1, the peak demand for electricity is only 15.02 MW (down by 49.84%). The addition of the natural gas network with the emission cost of 799 $/day is remarkably effective considering the total operation cost for the day is down by 29%, in which total system losses fall from 8.48 to 5.21 MW, as shown in Table VI. This can be explained by the fact that natural gas prices remain unchanged and are always lower than electricity prices. Therefore, when electricity prices are high, the system uses natural gas to achieve a lower cost.

3) Case 3

The MEN structure in Case 3 considers the addition of solar (PV generation and SHE) and WP sources. The input energy is illustrated in Fig. 9(c). The additional heat from the SHE in EHs 1, 2, 3, and 6 considerably alters the energy demands. Compared with Case 2, the peak demand at 7 p.m. is only 14.02 MW (down by 6.65%), especially at 12 p. m.. The total renewable energy discharged to the system is the highest when every PV and SHE provide the maximum capacity of 0.5 and 0.25 MW (WP is only allocated 0.13 MW to the system), respectively. Then, the total energy demand from the system drops from 12.21 to 11.75 MW. The results listed in Table VI show that, compared with Case 2, the MEN in Case 1 with solar and wind leads to a significant improvement in operation efficiency (where the total operation cost falls by 10.3%). In particular, the total capacity loss during the operation is down by 15.16%. Although the investment costs remain high, the effectiveness of these sources in reducing environmental pollution is also reduced from 799 to 688 $/day.

4) Case 4

Case 4 assesses the simultaneous impacts of solar, wind, and ESSs on the optimal performance of the MEN. Figure 9(d) shows that the total power purchased from utilities is significantly reduced compared with other operation cases, particularly during peak hours. Specifically, the maximum energy is 12.1 MW at 7 p. m. (down by 13.69% compared with Case 3). The optimal charging/discharging energy of the ESSs for EHs 2, 3, and 6 is shown in Fig. 10 with a rated power of 0.45 kW and a storage capacity of 4.2 MW. Specifically, at EH 2, ES stores energy during the time slots with low electricity prices (from 1 a. m. to 4 a. m.), and the electricity is discharged to the electricity network during the time slots with high energy costs (from 7 a. m. to 9 a. m.). During the remaining time slots, ES does not store or transmit energy to the network to reduce losses. At EHs 3 and 6, the working mode is the same as shown in Fig. 10(a). The charging/discharging mode of HS at EH 6 is shown in Fig. 10(b). HS is charged with a total capacity of 0.43 MW at 12 a.m., releasing 0.41 MW at 6 p.m.. This can be explained by the working mode of HS, which depends on the optimal working mode of the MEN.

In addition, the location of EH 6 is the furthest from the source. Therefore, not only the ES but also the HS equipped at EH 6 operates only at a particular time. Figure 10(c) shows the charging/discharging mode of the ES fits on EHs 2 and 6. Similar to the HS, the operation mode of the CS does not depend considerably on fluctuations in electricity prices. However, cooling demand for the load on all EHs is mainly provided by two devices (AC and ACh), the efficien-

cies of which are lower than those of the heat converters. Therefore, the CS is more involved in the optimal operation mode of the system. Specifically, at EH 2, CS has the total charging and discharging capacities of 1.79 MW/day and 1.71 MW/day, respectively. At EH 6, the full capacity is 1.86 MW/day and the released capacity is 1.78 MW/day. The additions of ESSs, including those for electricity, heat, and cooling, increase the operation efficiency of the model. The total operation cost in this case is the lowest, as shown in Table VI. Therefore, the MEN that includes electricity, natural gas, solar, and wind is more efficient than in the other three cases.

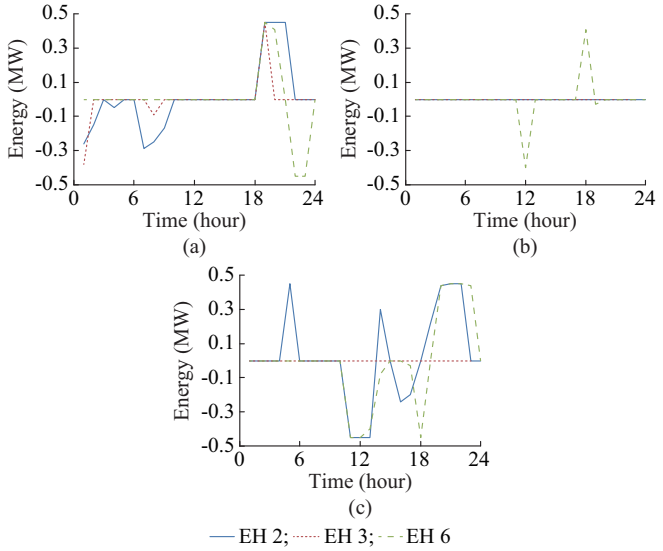

Fig. 10. Charging and discharging energies of ESS. (a) ES. (b) HS. (c) CS.

5) Discussion

Based on the previous calculation results, some primary analysis can be performed.

The combined use of many EHs to form the MEN structure (solar, wind, and ESS) responds appropriately and flexibly to the diversity of additional loads. The optimal calculation results show that the optimal model can respond properly to the changes in electricity costs and other energy prices. Simultaneously, the model allows for the adjustment of renewable energies over time and season.

Comparisons of four cases for the MEN clarify the role and impact of ESS, solar, and wind on the performance of the model in terms of reductions in total operation costs as shown in Table VI, losses, and pollution. Specifically, we find that the total operation cost in Case 4 drops by 35.84% compared with Case 1, and the total loss in Case 4 is reduced by 60.14%. Thus, it can be concluded that cutting down electricity demands during peak hours helps meet the urgent upgradation requirements of power distribution networks.

Additional investment costs for natural gas networks, PV, SHE, and wind turbine equipment are quite high but can be offset by the operation cost savings of the MEN. The results demonstrate that the proposed MEN model can significantly contribute to future research of multi-energy systems that integrate renewable energies and ESSs.

VI. Conclusion

Using the EH model in an MEN, this study proposes a methodology for the optimal operation and coordination between the electricity network and natural gas network that integrate solar, wind, and ESS. Each EH is considered as a node in the combined energy system to perform energy conversion.

This study analyzes the energy consumption of the whole system and emission amounts through four cases to assess the impacts of DERs and ESS on the performance of the MEN. Compared with the traditional thermal-power operation, the proposed model yields higher overall benefits and provides a theoretical basis for optimizing the operation of the systems with different forms of energy.

The cas study results show that the structures of the EHs used in the energy network have a significant effect on operation efficiency. Further research should be conducted on the optimal operation strategy for the different EHs and the optimization of the EH structures in the entire energy network. In addition, when investigating the effects of distributed energies, including solar, wind, and new energy storage devices, researchers should consider optimizing the locations and capacities of those devices for optimal network performance and efficiency improvement.

References

[1] M. Geidl, G. Koeppel, P. Favre-Perrod *et al.*, "Energy hubs for the future," *IEEE Power and Energy Magazine*, vol. 5, no. 1, pp. 24-30, Jan. 2007.

[2] T. Krause, G. Andersson, K. F. Hlich *et al.*, "Multiple-energy carriers: modeling of production, delivery, and consumption," *Proceedings of the IEEE*, vol. 99, no. 1, pp. 15-27, Jan. 2011.

[3] X. Xu, H. Jia, D. Wang *et al.*, "Hierarchical energy management system for multi-source multi-product microgrids," *Renewable Energy*, vol. 78, pp. 621-630, Jun. 2015.

[4] Y. Zha, T. Zhang, Z. Huang *et al.*, "Analysis of Energy Internet key technologies," *Scientia Sinica Informationis*, vol. 44, no. 6, pp. 702-713, Jun. 2014.

[5] Q. Sun, R. Han, H. Zhang *et al.*, "A multiagent-based consensus algorithm for distributed coordinated control of distributed generators in the Energy Internet," *IEEE Transactions on Smart Grid*, vol. 6, no. 6, pp. 3006-3019, Nov. 2015.

[6] Y. Ma, X. Wang, X. Zhou *et al.*, "An overview of Energy Internet," in *Proceeding of IEEE 2016 Chinese Control and Decision Conference*, Yinchuan, China, May 2016, pp. 6212-6215.

[7] T. Ha, Y. Zhang, V. V. Thang *et al.*, "Energy hub modeling to minimize residential energy costs considering solar energy and BESS," *Journal of Modern Power Systems and Clean Energy*, vol. 5, no. 3, pp. 389-399, Apr. 2017.

[8] T. T. Ha, Y. Zhang, J. Hao *et al.*, "Optimal operation of energy hub with different structures for minimal energy usage cost," in *Proceedings of the 2017 IEEE International Conference on Power and Renewable Energy*, Chengdu, China, May 2017, pp. 31-36.

[9] M. Geidl and G. Andersson, "A modeling and optimization approach for multiple energy carrier power flow," in *Proceedings of IEEE Russia Power Tech*, St. Petersburg, Russia, Jun. 2005, pp. 1-7.

[10] M. Geidl. (2017, May). Integrated modeling and optimization of multi-carrier energy systems. [Online]. Available: https://www.research-collection.ethz.ch/bitstream/handle/20.500.11850/123494/eth-29506-02.pdf

[11] M. Arnold, R. Negenborn, G. Andersson *et al.*, "Distributed predictive control for energy hub coordination in coupled electricity and gas networks," *International Journal of Control Automation and Systems*, vol. 42, pp. 235-273, Nov. 2010.

[12] M. Moeini-Aghtaie, A. Abbaspour, M. Fotuhi-Firuzabad *et al.*, "A decomposed solution to multiple-energy carriers optimal power flow," *IEEE Transactions on Power Systems*, vol. 29, no. 2, pp. 707-716, Mar. 2014.

[13] M. Geidl and G. Andersson, "Optimal power flow of multiple energy

carriers," *IEEE Transactions on Power Systems*, vol. 22, no. 1, pp. 145-155, Feb. 2007.
[14] M. Moeini-Aghtaie, P. Dehghanian, M. Fotuhi-Firuzabad *et al*., "Multi-agent genetic algorithm: an online probabilistic view on economic dispatch of energy hubs constrained by wind availability," *IEEE Transactions on Sustainable Energy*, vol. 5, no. 2, pp. 699-708, Jan. 2013.
[15] M. Moeini-Aghtaie, A. Abbaspour, M. Fotuhi-Firuzabad *et al*., "A decomposed solution to multiple-energy carriers optimal power flow," *IEEE Transactions on Power Systems*, vol. 29, no. 2, pp. 707-716, Mar. 2014
[16] B. Lu and M. Shahidehpour, "Short-term scheduling of battery in a grid-connected PV/battery system," *IEEE Transactions on Power Systems*, vol. 20 no. 2, pp. 1053-1061, May 2005.
[17] M. Rastegar, M. Fotuhi-Firuzabad, and M. Lehtonen, "Home load management in a residential energy hub," *Electric Power Systems Research*, vol. 119, pp. 322-328, Feb. 2015.
[18] M. C. Bozchalui, S. A. Hashmi, H. Hassen *et al*., "Optimal operation of residential energy hubs in smart grid," *IEEE Transactions on Smart Grid*, vol. 3, no. 4, pp. 1755-1766, Oct. 2012.
[19] X. Shen, Y. Han, S. Zhu *et al*., "Comprehensive power-supply planning for active distribution system considering cooling, heating and power load balance," *Journal of Modern Power Systems and Clean Energy*, vol. 3, no. 4, pp. 485-493, Nov. 2015.
[20] M. Liu, Y. Shi, and F. Fang, "Combined cooling, heating and power systems," *Renewable and Sustainable Energy Reviews*, vol. 35, pp. 1-22, Jul. 2014.
[21] A. Maroufmashat, A. Elkamel, M. Fowler *et al*., "Modeling and optimization of a network of energy hubs to improve economic and emission considerations," *Energy*, vol. 93, pp. 2546-2558, Dec. 2015.
[22] Y. Li, Z. Li, F. Wen *et al*., "Privacy-preserving optimal dispatch for an integrated power distribution and natural gas system in networked energy hubs," *IEEE Transactions on Sustainable Energy*, vol. 10, no. 4, pp. 2028-2038, Oct. 2019.
[23] Y. Huang, W. Zhang, K. Yang *et al*., "An optimal scheduling method for multi-energy hub systems using game theory," *Energies*, vol. 12, no. 12, pp. 2270-2290, Jun. 2019.
[24] H. R. Gholinejad, A. Loni, J. Adabi *et al*., "A hierarchical energy management system for multiple home energy hubs in neighborhood grids," *Journal of Building Engineering*, vol. 28, pp. 1-10, Mar. 2020.
[25] M. Jadidbonab, B. Mohammadi-Ivatloo, M. Marzband *et al*., "Short-term self-scheduling of virtual energy hub plant within thermal energy market," *IEEE Transactions on Industrial Electronics*, vol. 6, no. 4, pp. 3124-3136, Apr. 2021.
[26] M. Nazari-Heris, M. A. Mirzaei, and B. Mohammadi-Ivatloo, "Economic-environmental effect of power to gas technology in coupled electricity and gas systems with price-responsive shiftable loads," *Journal of Cleaner Production*, vol. 244, pp. 1-9, Jan. 2020.
[27] M. Marzband, F. Azarinejadian, M. Savaghebi *et al*., "Smart transactive energy framework in grid-connected multiple home microgrids under independent and coalition operations," *Renewable Energy*, vol. 126, pp. 95-106, Oct. 2018.
[28] R. Das, Y. Wang, G. Putrus *et al*., "Multi-objective techno-economic-environmental optimization of electric vehicle for energy services," *Applied Energy*, vol. 257, pp. 1-9, Oct. 2019.
[29] M. A. Mirzaei, A. S. Yazdankhah, B. Mohammadi-Ivatloo *et al*., "Integration of emerging resources in IGDT-based robust scheduling of combined power and natural gas systems considering flexible ramping products," *Energy*, vol. 189, pp. 1-8, Dec. 2019.
[30] M. Mohammadi, Y. Noorollahi, B. Mohammadi-Ivatloo *et al*., "Energy hub: from a model to a concept – a review," *Renewable and Sustainable Energy Reviews*, vol. 80, pp. 1512-1527, Dec. 2017.
[31] S. Pazouki, M. R. Haghifam, and A. Moser, "Uncertainty modeling in optimal operation of energy hub in presence of wind, storage and demand response," *International Journal of Electrical Power & Energy Systems*, vol. 61, pp. 335-345, Oct. 2014.
[32] A. Parisio, C. D. Vecchio, and A. Vaccaro, "A robust optimization approach to energy hub management," *International Journal of Electrical Power & Energy Systems*, vol. 42, no. 1, pp. 98-104, Nov. 2012.
[33] A. Martinez-Mares and C. R. Fuerte-Esquivel, "A unified gas and power flow analysis in natural gas and electricity coupled networks," *IEEE Transactions on Power Systems*, vol. 27, no. 4, pp. 2156-2166, Nov. 2012.
[34] S. Mokhatab, W. A. Poe, and J. G. Speight, *Handbook of Natural Gas Transmission and Processing*. Burlington: Elsevier, 2012.
[35] Maryland Public Service Commission. (2016, Oct.). Gas commodity fact sheet for Maryland Public Service Commission. [Online]. Available: http://www.psc.state.md.us/gas/
[36] T. T. Ha, Y. Zhang, J. Hao *et al*., "Energy hub's structural and operational optimization for minimal energy usage costs in energy systems," *Energies*, vol. 11, no. 4, p. 707, Mar. 2018.
[37] Maryland Public Service Commission. (2016, Oct.). Home electricity price. [Online]. Available: http://www.opc.state.md.us/ConsumerCorner/Electricity.aspx
[38] A. Brooke, D. Kendrick, and A. Meeraus, *GAMS: a User's Guide*. Washington DC: AMS Development Corporation, 2003.

Thanhtung Ha received the B.Sc. and M.Sc. degrees in the Department of Electric Power Systems at Thai Nguyen University of Technology (TNUT), Thai Nguyen, Vietnam, in 2009 and 2012, respectively. He received the Ph. D. degree in electrical engineering at South China University of Technology, Guangzhou, China, in 2019. His research interests include analysis and control of operation of energy system.

Ying Xue received the B. Eng. degree in electrical engineering from the Huazhong University of Science and Technology, Wuhan, China, and the University of Birmingham, Birmingham, U.K., in 2012, and the Ph.D. degree in electrical engineering from the University of Birmingham, in 2016. He is currently a Lecturer with the University of Birmingham. His research interests include HVDC modeling and control.

Kaidong Lin received the B.Sc. degree in the Department of Electrical Engineering and Automation, China University of Mining and Technology, Xuzhou, China, in 2017. He is currently pursuing Ph.D. degree in South China University of Technology, Guangzhou, China. His research interests include the analysis and control of the operation of energy system, load forecasting, and power market.

Yongjun Zhang received the Ph.D. degree in power system and its automation from the South China University of Technology, Guangzhou, China, in 2004, where he was an Assistant Professor from 2005 to 2012. Since 2012, he has been a Professor at the same university. His research interests include power system reactive power optimization, voltage control, smart energy system, and HVDC transmission.

Vu Van Thang received the B.Sc. and M.Sc. degrees in the Department of Electric Power Systems, Thai Nguyen University of Technology (TNUT), Thai Nguyen, Vietnam, in 2001 and 2007, respectively. He received the Ph. D. degree at the Hanoi University of Science and Technology (HUST), Hanoi, Vietnam, in 2015. He is currently a Lecturer in the Department of Electric Power System at TNUT. His research interests include optimizing energy systems, distributed generation and distribution system in deregulated electricity markets.

Thanhha Nguyen received the Ph.D. degree in the Hanoi University of Science and Technology (HUST), Hanoi, Vietnam, in 2003. From 2010, he is an Assistant Professor in Thai Nguyen University, Thai Nguyen, Vietnam. His research interests include analysis and control of operation of energy system and computer applications.